Green photoluminescence of partially oxidized and fully oxidized Zn films

Bao-gai Zhai, Jun-shen Li, Yuan Ming Huang*

School of Mathematics and Physics, Changzhou University, Jiangsu 213164, China
(*Received 18 August 2016; accepted 2 November 2016*)

Zn thin films were deposited onto glass and quartz substrates using the magnetron-sputtering technique. Zn-rich ZnO thin films were prepared by partially oxidizing the magnetron-sputtered Zn films at room temperature in air while O-rich ZnO thin films were prepared by fully oxidizing the Zn films at 600°C in an air-filled furnace. The crystal structures and photoluminescence (PL) of Zn-rich and O-rich ZnO thin films were analyzed with X-ray diffractometer and fluorescence spectrophotometer, respectively. The PL spectrum of the Zn-rich ZnO film consists a ultraviolet emission band centered at about 367 nm and a green emission band peaked at around 535 nm. As a contrast, the PL spectrum of the O-rich ZnO film exhibits a green emission band peaked at around 500 nm with its ultraviolet emission band heavily suppressed. Using the density functional theory in the frame work of meta general gradient approximation, the bandstructures and density of states were calculated for Zn-rich ZnO ($ZnO_{0.99}$ and $ZnO_{0.98}$) and O-rich ZnO ($Zn_{0.98}O$). It was found that the defect energy level positions of oxygen vacancies in the bandgap of ZnO are dependent on the concentration of oxygen vacancies, the deep donor traps of oxygen vacancy in the bandgap of ZnO are determined at E_V + 0.76 eV for $ZnO_{0.99}$ and at E_V + 0.84 eV for $ZnO_{0.98}$. As a contrast, Zn vacancy in $Zn_{0.98}O$ introduces only shallow defect energy levels, which are very close to the valence band maximum. In the light of the calculated bandstructures, the origins of the green PL band from both Zn-rich ZnO films and O-rich films can be attributed to the oxygen vacancy in ZnO lattice.

Keywords: ZnO thin film; Photoluminescence; Bandstructure; Zn vacancy; Oxygen vacancy

1. Introduction

Due to its wide bandgap (3.37 eV) and large exciton binding energy (60 meV), ZnO is considered as one of the most promising semiconductor materials for light emitting diodes, solar cells, photocatalysts, etc [1-6]. Among its rich optical properties, the photoluminescence (PL) of ZnO has been intensively investigated. Generally speaking, the room temperature PL spectrum of ZnO nanostructures consists of two signature peaks. The first signature peak is a sharp free-exciton ultraviolet band that usually centers on 380 nm, which can be attributed to the band-edge emission due to the recombination of free excitons. The second signature peak is a broad green luminescence band. In undoped ZnO, the green luminescence band peaking at about 496 nm (2.5 eV) usually dominates the defect-related part of the PL spectrum. For example, we recorded green emission band with its peak at 500 nm for the ZnO nanorods and nanowires that were synthesized by Zn vapor condensation in air [7,8]. In spite of the intensive studies so far, the recombination center of the green PL of ZnO is poorly understood [9-13]. In the early studies performed in 1950s and 1960s, the nature of the visible emission was unambiguously attributed to copper impurities, but later intrinsic defects such as interstitial Zn ions or oxygen vacancies were assumed to be the recombination centers of the green PL band [9-11]. In the past 20 years, some authors suggested the oxygen vacancy a source of the green luminescence [14,15], whereas others attribute it to the Zn vacancy [16] and oxygen antisite [17]. For example, van Dijken *et al* assumed that the visible emission is due to a transition of an electron from a level close to the conduction band edge to a deeply trapped hole in the bulk of the ZnO particle [15]; Zhao *et al* concluded that the zinc vacancy is responsible for the observed deep-level emission [16]; whereas Lin *et al* proposed that the green emission occurs from the local level composed by oxygen antisite [17]. It is clear that the origin of the green luminescence in ZnO has been a topic of intensive discussion.

The lack of a reliable method to determine the locations of intrinsic defect levels in the bandgap of ZnO has led to various speculative models and mechanisms on the green PL band. A literature review reveals that first principles density functional theory (DFT) calculations have been widely used in most studies in order to accurately determine the locations of intrinsic defect levels in the bandgap of ZnO. However, it is well established that neither the calculated bandstructures nor the calculated bandgaps in the framework of DFT are not in good consistency with experimental values, no matter whether the local density approximation (LDA) or the generalized gradient approximation (GGA) is employed to describe the exchange-correlation functional in ZnO. A simple correction scheme is to shift the conduction band minimum upward so that the calculated bandgap of ZnO agrees with an experimental value. Defect-induced electronic states are considered to follow this shift. Such kind of shortcomings in DFT based calculations makes it hard to correctly and precisely determine the defect energy levels of intrinsic point defects in ZnO.

The controversy could be alleviated, at least in part, if one can precisely determine the defect energy levels of intrinsic point defects in the bandgap of ZnO. It was recently reported that first-principles DFT calculations in the framework of meta GGA can give the correct bandgap for ZnO [18,19]. In order to shed new light on the origin of the green luminescence in ZnO, this work aims to combine the DFT based bandstructure calculations with experimental PL measurements of Zn-rich ZnO and oxygen-rich ZnO (O-rich ZnO). On one hand, Zn-rich ZnO and O-rich ZnO thin films were deposited onto glass

*Corresponding author. Email: dongshanisland@126.com

or quartz substrates, and their green PL properties were investigated. On the other hand, the bandstructures of Zn-rich ZnO and O-rich ZnO were derived with DFT calculations in the framework of meta GGA for the accurate determination of the defect levels of oxygen and Zn vacancies in the bandgap of ZnO. The correlation between the green emissions and the defect energy levels suggests that the oxygen vacancies are the most likely candidates for the recombination centers involved in the green luminescence of ZnO.

2. Experimental and computational details

Glass plates wee selected as the substrates to grow Zn thin films. Before use, the substrates were ultrasonically cleaned in liquid detergent, acetone, ethanol and distilled water for 15 min each, and then were dried in blowing Ar gas. Zn-rich thin films were deposited onto the glass substrates by reactive RF magnetron sputtering technique. A high-purity Zn target (99.99%) was used as the Zn source in the magnetron sputtering, and high-purity Ar (99.99%) was selected as the sputtering gas. In the vacuum chamber, the distance between the Zn target and the glass substrate was 100 mm. The base pressure in the vacuum chamber was 4×10^{-4} Pa, and the working pressure in the vacuum chamber was 0.8 Pa. The RF sputtering power was adjusted to be 100 W. The substrate was not electrically heated during deposition. The sputtering duration was 15 min. Non-stoichiometric ZnO films were used in this study. Zn-rich ZnO thin film was obtained after the magnetron sputtered Zn films were exposed to air at room temperature for a couple of weeks. The partially oxidized Zn film was also denoted as Zn-rich ZnO film, in which the population density of oxygen vacancy should dominate over the population density of Zn vacancies. Furthermore, O-rich ZnO was obtained by annealing the magnetron sputtered metallic Zn film in an air-filled furnace at 600°C for 4 h. The long term heating could completely convert the Zn films into ZnO. The fully oxidized Zn thin film could be called as O-rich ZnO thin film, in which the population density of Zn vacancy should dominate over the population density of oxygen vacancies.

XRD (D/max 2500 PC, Japan) was utilized to analyze the crystal structures of the samples. A copper target was utilized to generate the X-ray (λ = 0.154 nm). The PL spectra of the samples were recorded with a spectrophotometer (Tianjin Gangdong Ltd., China). The 325-nm laser line from a helium-cadmium laser was utilized as the excitation source for the PL measurement. More details on the instruments and their operating parameters were described elsewhere [2-5,7,8].

Using the DFT module of the Quantumwise Atomistix ToolKit 11.8 package, first-principles DFT calculations were performed to derive the of the bandstructures of defect-free ZnO, Zn-rich ZnO and O-rich ZnO. The exchange-correlation functional was treated within the meta GGA scheme [18,19]. The exchange potential in the meta GGA scheme was described by the modified Becke and Johnson exchange potential [18]. For Brillouin zone integrations, a $5\times5\times5$ grid was used following a Monkhorst-Pack scheme. To model oxygen vacancies in ZnO matrix, we built up the $(4\times4\times3)$ supercell for ZnO with the lattice constants of a = 0.32495 nm and c = 0.52069 nm. There were 96 O sites and 96 Zn sites in the supercell. When one O site near the center of the supercell was removed, about 1% oxygen vacancies were generated in ZnO. Consequently, the ZnO with 1% oxygen vacancies was denoted as $ZnO_{0.99}$ in this report. In order to study oxygen vacancy concentration dependent electronic structures, a $(3\times3\times3)$ supercell was built in a similar way for $ZnO_{0.98}$ by removing one of 54 O sites from the center of the supercell. Finally, a $(3\times3\times3)$ supercell was built for $Zn_{0.98}O$ when one of the 54 Zn sites was removed from the center of the supercell. Double zeta double polarized basis sets were chosen for each element. The mesh cut-off energy was set to be 100 Hartree. The convergence tolerance of the calculation was 4×10^{-5} eV of the total energy.

3. Results and discussion

Fig. 1 depicts the XRD spectra of the partially oxidized Zn thin film (curve *a*) and the fully oxidized Zn film (curve *b*). As shown in Fig. 1(a), the diffraction peaks of partially oxidized Zn film are located at 36.29°, 38.99°, 43.23°, 54.34° and 70.4°, which can be assigned to the (002), (100), (101), (102) and (103) crystallographic planes of hexagonal Zn (JCPDS No. 04-0381). A detailed analysis of curve a reveals that the presence of ZnO in the partially oxidized Zn film since, as labeled with the open circles upon curve *a*, the weak diffraction peaks at 31.62°, 34.35°, 56.58° and 62.84° are the characteristics of ZnO. Thus curve a has confirmed the partial oxidization of the as-prepared Zn film after having been stored in air for a couple of weeks. The diffraction peaks in Fig. 1(b) are located at 2θ = 31.62°, 34.35°, 36.22°, 47.45°, 56.58°, 62.84° and 67.91°. As discussed previously, these diffraction peaks can be assigned to the (100), (002), (101), (102), (110), (103) and (112) planes of wurtzite ZnO (JCPDS No. 36-1451), respectively [2-5]. According to the Bragg diffraction equation, the lattice constants a and c of the ZnO microcrystals were derived to be 0.326 and 0.521 nm, respectively, which are in good agreement with the standard lattice constants of wurtzite ZnO. Therefore, curve b has demonstrated that the as-prepared Zn films are completely turned into ZnO films after heat treatment at 600°C in an air-filled furnace for 4 h.

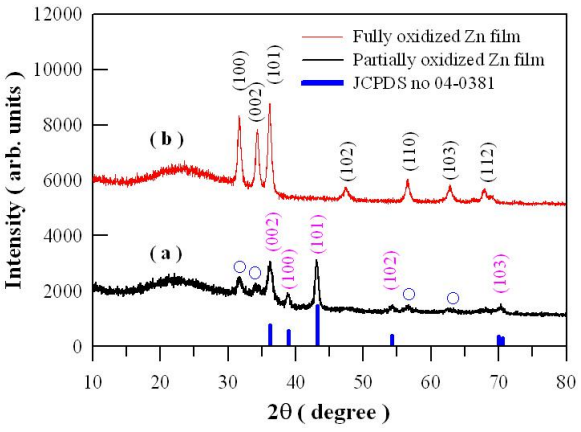

Fig. 1 XRD spectra of Zn-rich ZnO film (a) and O-rich ZnO

film (b).

Fig. 2 illustrates the PL spectra of the partially oxidized Zn film (top panel) and fully oxidized Zn film (bottom panel). As shown in the top panel, the PL spectrum of the partially oxidized Zn film is composed of an intense ultraviolet PL band with its peak centered at around 367 nm and a broad green PL band with its peak located at around 535 nm. The peak at 367 nm (3.38 eV) can be ascribed to the near band-edge emission of ZnO since it is commonly accepted that the ultraviolet emission is the characteristic emission of ZnO and arises from the band-edge transition or exciton recombination. As a contrast, it remains puzzling on the luminescence center of green PL band. As illustrated in the top panel, the green PL band of the partially oxidized Zn film can be decomposed into two Gaussian components. The first Gaussian component is peaked at 500 nm while the second Gaussian component is centered at 533 nm. The bottom panel in Fig. 2 represents the typical PL spectrum of the fully oxidized Zn film on quartz plate. It is obvious that the PL spectrum of the fully oxidized Zn film is characteristic of a green PL band, whose peak is located at about 496 nm. We have to note that the broad PL band at around 400 nm in the bottom panel comes from the quartz substrate since some of the excitation photons (i.e, the 325 nm laser beam) can pass through the ZnO thin film to excite the defects in the quartz plate. The other characteristic of the PL spectrum of the fully oxidized Zn film is that its ultraviolet emission band is heavily suppressed. A comparison of the two PL curves in Fig. 2 shows that the PL spectrum of the fully oxidized Zn film is different from that of the partially oxidized Zn film.

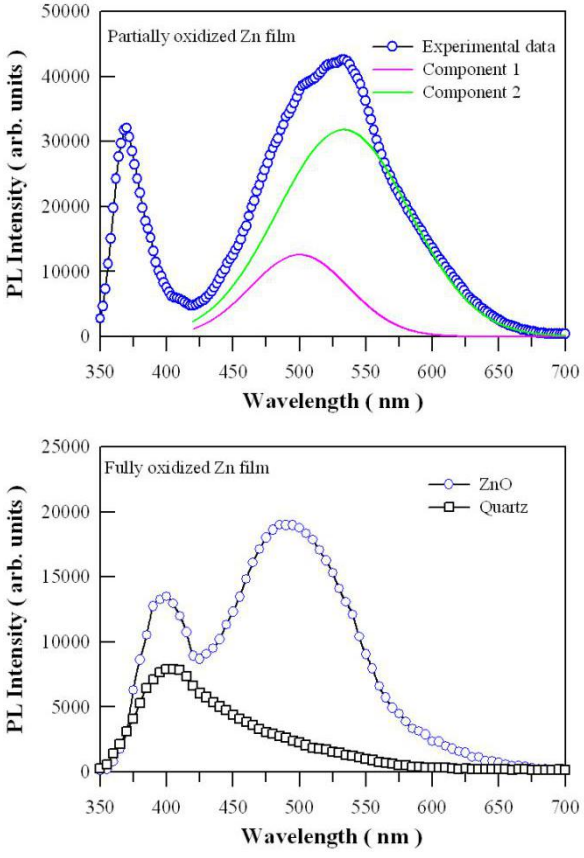

Fig. 2 PL spectra of Zn-rich ZnO and O-rich ZnO films.

The intrinsic point defects, along with their complexes, should play a profound role in the optical behaviors of ZnO. There are six kinds of native point defects in ZnO, examples include oxygen vacancy, Zn vacancy, oxygen interstitial, Zn interstitial, oxygen antisite and Zn antisite. As mentioned before, the origin of the ubiquitous green luminescence remains controversial and has been attributed to several native defects such as oxygen vacancy [14,15], Zn vacancy [16], Zn interstitials and Zn antisite [17]. Among these native defects, the Zn interstitial, which has been generally considered to act as a shallow donor, can be excluded from the luminescence center of the green emissions due to the following reasons: (i) the defect energy levels of Zn interstitial is about 30 meV below the conduction band minimum [20,21]; and (ii) most studies conclude that the Zn interstitial has a high formation energy [12]. Thus, Zn interstitial should be excluded from consideration as the luminescence center of the green PL band. Zn antisite and oxygen antisites can also be ruled out. According to DFT calculations, the oxygen interstitial, Zn antisite and oxygen antisite defects are unlikely the cause of the green PL band since they have too high formation energies to occur in any significant concentrations [22,23]. Therefore, neither the interstitials nor antisites of oxygen and Zn are likely the luminescence center for the green emission of ZnO, leaving the possible candidates to oxygen vacancy and Zn vacancy. That is the reason why Kohan et al concluded that both the Zn and O vacancies are the relevant defects in ZnO, according to their first-principles study [24].

During the past years, oxygen vacancies have been assumed to be the most likely candidates for the recombination centers involved in the visible luminescence of ZnO. As an intrinsic donor in ZnO, oxygen vacancy can occur in three different charge states: the neutral state which has captured two electrons and is neutral relative to the lattice, the singly ionized state, and the doubly ionized state which did not trap any electron and is doubly positively charged with respect to the lattice. Vanheusden *et al* proposed that the singly ionized oxygen vacancy is responsible for the green emission in ZnO [14]; van Dijken *et al* assumed that the visible emission is due to a transition of an electron from a level close to the conduction band edge to a deeply trapped hole in the bulk of the ZnO particle [15]; Leiter *et al* identified the oxygen vacancy as the defect responsible for the structureless green emission band in ZnO [23]. In order to check if the oxygen vacancy is the luminescence center of the green PL in ZnO, the knowledge on the exact positions of the defect energy level in the bandgap of ZnO becomes critically important. Fig. 3 displays the calculated bandstructures of the perfect ZnO (upper panel) and Zn-rich (i..e, oxygen deficient) $ZnO_{0.99}$ (lower panel). As shown in the upper panel of Fig. 3, the perfect ZnO is a direct semiconductor with its bandgap of 3.40 eV. The bang gap value from the first-principles DFT calculations is in good agreement to the experimental value of ZnO (3.37 eV). The bottom panel of Fig. 3 indicates that the bandgap of the Zn-rich and oxygen deficient $ZnO_{0.99}$ is

direct but its bandgap is widened to 3.517 eV, indicating that the bandstructures are changed as 1% oxygen sites are removed from the perfect ZnO. More importantly, one defect level is introduced in the bandgap of $ZnO_{0.99}$, As shown by the red energy levels in the lower panel of Fig. 3, the defect level of oxygen vacancy is located at about 0.762 eV above the valence band maximum (E_V + 0.762 eV). In the light of the calculated bandstructures, the recombination of electron in the conduction band with the hole-like oxygen vacancy will lead to the blue emission at about 450 nm. When compared to the green PL band in the top panel of Fig. 2, the predicted blue emission at 450 nm agrees roughly to the green PL bands of Zn-rich ZnO films.

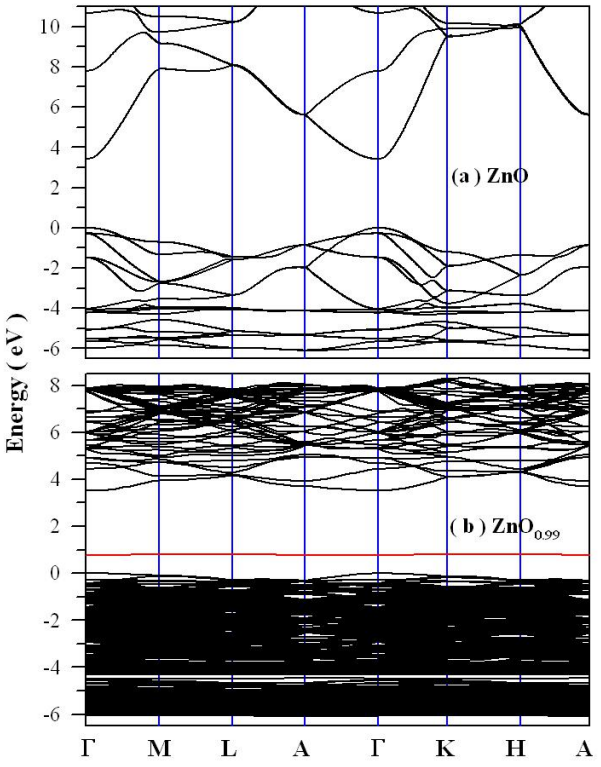

Fig. 3 DFT calculated bandstructures of perfect ZnO (upper panel) and oxygen-deficient $ZnO_{0.99}$ (lower panel).

In order to study the influence of oxygen vacancy concentration on the defect energy level position in the bandgap of ZnO, we calculated the bandstructures and density of states for $ZnO_{0.98}$. Fig. 4 shows the DFT calculated bandstructures and density of states of Zn-rich (i.e., oxygen deficient) $ZnO_{0.98}$. As shown in Fig. 4(a), the oxygen-deficient $ZnO_{0.98}$ is still a direct semiconductor but its bandgap is widened furthermore to 3.600 eV. Thus the concentration of oxygen vacancy in ZnO affects the bandgap of ZnO. When compared to Fig. 3, we can conclude that the bandgap of Zn-rich, oxygen deficient ZnO is enlarged as the concentration of oxygen vacancy in ZnO increases. In particular, it has been observed that the defect level of the oxygen vacancy is located at E_V + 0.668 eV. The defect energy level position of the oxygen vacancy can be seen clearly in Fig. 4(b). When compared to Fig. 3(b), it is clear that the defect energy level position of the oxygen vacancy is dependent on the defect concentration. The oxygen vacancy in ZnO is positively charged. When electron in the conduction band recombine with the hole-like oxygen vacancy, it will lead to the blue emission at about 423 nm.

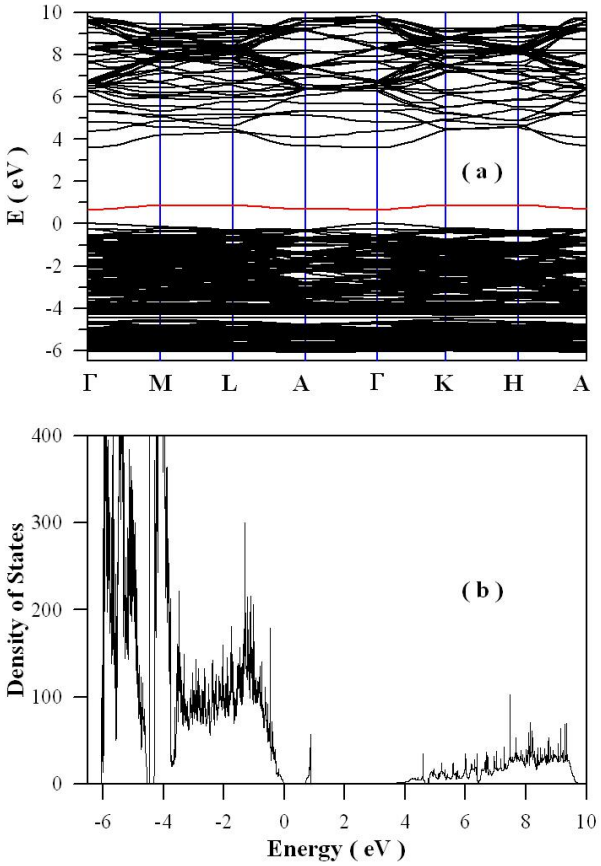

Fig. 4 DFT calculated bandstructures and density of states of Zn-rich and oxygen-deficient $ZnO_{0.98}$.

Fig. 5 shows the calculated bandstructures and density of states of O-rich (i.e., Zn deficient) Zn0.98O. The bandgap of $Zn_{0.98}O$, which is direct, can be measured from Fig. 5(a). The calculated bandgap value is 3.511 eV for $Zn_{0.98}O$. It is also noteworthy that the bandgap of O-rich, Zn deficient $Zn_{0.98}O$ is nearly clean, suggesting that no deep defect levels are introduced in the bandgap of the O-rich and Zn deficient $Zn_{0.98}O$. Thus it is safe for us to conclude that the point defect of Zn vacancy does not introduce any deep defect levels in the bandgap of ZnO. Detailed analysis of Fig. 5(b) reveals that the defect energy level position of Zn vacancy defect is very close to the valence band maximum, indicating that Zn vacancy works as a shallow acceptor. As reported by some researchers, it is widely accepted that Zn vacancy acts as the dominant compensating acceptor in n-type ZnO with a concentration of 10^{15}-10^{16} cm^{-3} [25], but its energy position remains highly controversial. For instance, Lany *et al* and Janotti and van de Walle regarded Zn vacancy as a deep acceptor in terms of their first-principles theoretical calculations [26, 27], and they correlated the Zn vacancy with the green band emissions of ZnO [27,28]. Moreover, Zhao *et al* concluded that the Zn vacancy is responsible to the observed deep-level emission [16]. As a contrast, some reports suggested that the Zn vacancy holds a shallow acceptor state, which is 90-130 meV above the valence band maximum [29,30]. For example, Park *et al* and Travlos *et al* linked the Zn

vacancy shallow acceptor to the optical transition of free electron to neutral acceptor at around 3.31eV [31,32]. Although it is possible for Zn vacancy to be involved into the ultraviolet emission from ZnO, Fig. 5 shows that Zn vacancy is not possible to be the recombination center of the green emission band of ZnO. Considering the accuracy of electronic calculations for the Zn-rich and O-rich ZnO films, however, it is worth noting that the assignment of this green PL band is still controversial, and a lot of well-designed attempts are required in the future to elucidate the origin of the green PL from ZnO [32,33].

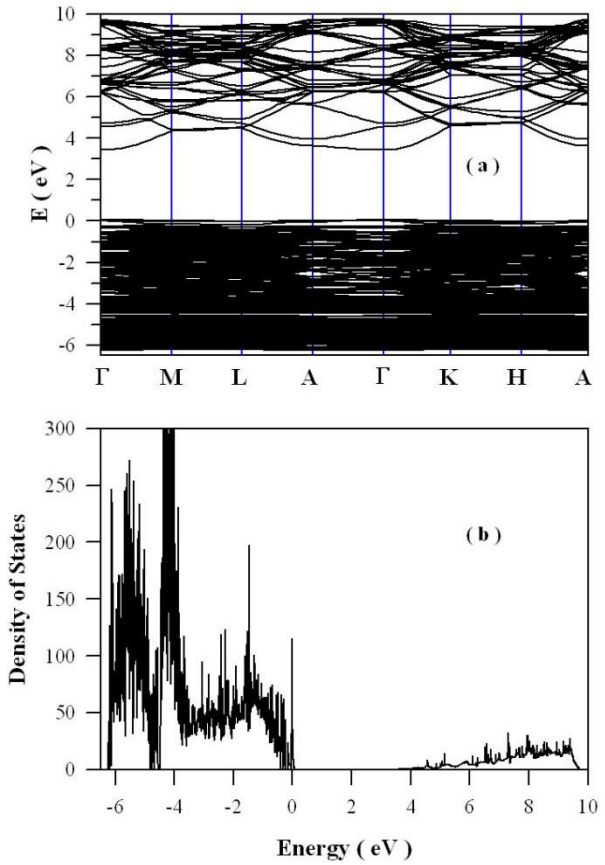

Fig. 5 The DFT calculated bandstructures and density of states of O-rich and Zn-deficient $Zn_{0.98}O$.

On the basis of the calculated bandstructures for Zn-rich ZnO and O-rich ZnO, we can assign the green PL bands from the Zn-rich ZnO and O-rich ZnO thin films to oxygen vacancies. Qualitatively speaking, both oxygen vacancies and Zn vacancies are present in the Zn-rich ZnO and O-rich ZnO thin films, although in Zn-rich ZnO films the population density of oxygen vacancy dominates over the population density of Zn vacancies and vice versa. Therefore, the difference in the peak positions of the green PL band in Fig. 2 can be caused by the difference in the oxygen vacancy concentration in the two kinds of ZnO films.

4. Conclusion

In short, Zn thin films were deposited onto glass and quartz substrates using the magnetron-sputtering technique. Zn-rich ZnO thin films were prepared by partially oxidizing the magnetron-sputtered Zn films at room temperature in air, O-rich ZnO thin films were prepared by fully oxidizing the Zn films at 600°C in an air-filled furnace. The PL spectra show that both the Zn-rich and O-rich ZnO films give green luminescence with noticeable difference in the peaks. It can be concluded that the two most common defects in ZnO are likely to be oxygen and Zn vacancies. Our DFT calculations indicate that the oxygen vacancies in ZnO are likely the luminescence center of the green PL from ZnO, and that the transition from the conduction band of ZnO to the deep trap level of oxygen vacancy can give the green emissions.

Acknowledgment

This work was financially supported by Natural Science Foundation of China under the Grant No 11574036.

References

[1] P. Klason, T.M. Børseth, Q.X. Zhao, B.G. Svensson, A.Y. Kuznetsov, P.J. Bergman, M. Willander, Temperature dependence and decay times of zinc and oxygen vacancy related photoluminescence bands in zinc oxide, Solid State Commun. 145 (2008) 321–326.

[2] Y.M. Huang, Q.L. Ma, B.G. Zhai, Controlled morphology of ZnO nanostructures by adjusting the zinc foil heating temperature in an air-filled box furnace, Mater. Chem. Phys. 147 (2014) 788–795.

[3] Y.M. Huang, Q.L. Ma, B.G. Zhai, Wavelength tunable photoluminescence of ZnO/porous Si nanocomposites, J. Lumin. 138 (2013) 157–163.

[4] Q.L. Ma, Y.M. Huang, Improved photovoltaic performance of dye sensitized solar cell by decorating TiO2 photoanode with Li-doped ZnO nanorods, Mater. Lett. 148 (2015) 171–173.

[5] Q.L. Ma, R. Xiong, B.G. Zhai, Y.M. Huang, Ultrasonic synthesis of fern ‐ like ZnO nanoleaves and their enhanced photocatalytic activity, Appl. Surf. Sci. 324 (2015) 842–848.

[6] Ü. Özgür, Ya.I. Alivov, C. Liu, A.Teke, M.A. Reshchikov, S. Doğan, V. Avrutin, S.J. Cho, H. Morkoç, A comprehensive review of ZnO materials and devices, J. Appl. Phys. 98 (2005) 041301–041313.

[7] Y.M. Huang, Q.L. Ma, B.G. Zhai, A simple method to grow one-dimensional ZnO nanostructures in air, Mater. Lett. 93 (2013) 266–268.

[8] Y.M. Huang, Q.L Ma, B.G. Zhai, Controlled morphology of ZnO nanostructures by adjusting the zinc foil heating temperature in an air-filled box furnace, Mater. Chem. Phys. 147 (2014) 788–795.

[9] E. Mollwo, Die wirkung von wasserstoff auf die leitfahigkeit und lumineszenz von zinkoxydkristallen, Z. Phys. 138 (1954) 478–488.

[10] F. van Craeynest, W. Maenhout-van der Vorst, W. Dekeyser, Interpretation of the yellow colour of heat treated ZnO powder, Phys. Status Solidi 8 (1965) 841–848.

[11] W. Maenhout-Van Der Vorst, F. van Craeynest, The Green Luminescence of ZnO, Phys. Status Solidi 9 (1965) 749–752.

[12] F. Oba, M. Choi, A. Togo, I. Tanaka, Point defects in ZnO: an approach from first principles, Sci. Technol. Adv. Mater. 12 (2011) 034302.

[13] C. Ton-That, L. Weston, M.R. Phillips, Characteristics of point defects in the green luminescence from Zn- and O-rich ZnO, Phys. Rev. B, 86 (2012) 115205.

[14] K. Vanheusden, W.L. Warren, C.H. Seager, D.R. Tallant, J.A. Voigt,

B.E. Gnade, Mechanisms behind green photoluminescence in ZnO phosphor powders, J. Appl. Phys. 79 (1996) 7983–7989.

[15] Q.X. Zhao, P. Klason, M. Willander, H.M. Zhong, W. Lu, J.H. Yang, Deep-level emissions influenced by O and Zn implantations in ZnO, Appl. Phys. Lett. 87 (2005) 211912.

[16] B. Lin, Z. Fu, Y. Jia, Green luminescent center in undoped zinc oxide films deposited on silicon substrates, Appl. Phys. Lett. 79 (2001) 944–946.

[17] A. Van Dijken, E.A. Meulenkamp, D. Vanmaekelberg, A. Meijerink, The Kinetics of the radiative and nonradiative processes in nanocrystalline ZnO particles upon photoexcitation, J. Phys. Chem. B 104 (2000) 1715–1723.

[18] F. Tran, P. Blaha, Accurate band gaps of semiconductors and insulators with a semilocal exchange-correlation potential, Phys. Rev. Lett. 102 (2009) 226401

[19] D. Koller, F. Tran, P. Blaha, Merits and limits of the modified Becke-Johnson exchange potential, Phys. Rev. B 83 (2011) 195134.

[20] D.C. Look, J. W. Hemsky, J. R. Sizelove, Residual native shallow donor in ZnO, Phys. Rev. Lett. 82 (1999) 2552–2555.

[21] J. Sann, J. Stehr, A. Hofstaetter, D. M. Hofmann, A. Neumann, M. Lerch, U. Haboeck, A. Hoffmann, C. Thomsen, Zn interstitial related donors in ammonia-treated ZnO powders, Phys. Rev. B 76 (2007) 195203.

[22] A. Janotti, C. G. Van de Walle, New insights into the role of native point defects in ZnO, Phys. Rev. B 76 (2007) 165202.

[23] F. Leiter, H. Alves, D. Pfisterer, N.G. Romanov, D.M. Hofmann, B.K. Meyer, Oxygen vacancies in ZnO, Physica B 340–342 (2003) 201–204.

[24] A. F. Kohan, G. Ceder, D. Morgan, First-principles study of native point defects in ZnO, Phys. Rev. B 61 (2000) 15019.

[25] F. Tuomisto, V. Ranki, K. Saarinen, D.C. Look, Evidence of the Zn vacancy acting as the dominant acceptor in n-type ZnO, Phys. Rev. Lett. 91 (2003) 205502.

[26] S. Lany, A. Zunger, Dopability, intrinsic conductivity, and nonstoichiometry of transparent conducting oxides, Phys. Rev. Lett. 98 (2007) 045501.

[27] A. Janotti, C.G. van de Walle, Native point defects in ZnO, Phys. Rev. B 76 (2007) 165202.

[28] H. Chen, S.L. Gu, K. Tang, S.M. Zhu, Z.B. Zhu, J.D. Ye, R. Zhang, Y.D. Zheng, Origins of green band emission in high-temperature annealed N-doped ZnO, J. Lumin.131 (2011) 1189–1192.

[29] A. Zubiaga, J.A. Garcia, F. Plazaola, F. Tuomisto, K. Saarinen, J.Z. Perez, V. Munoz-Sanjose, Correlation between Zn vacancies and photoluminescence emission in ZnO films, J. Appl. Phys. 99 (2006) 053516.

[30] E.H. Khan, M.H. Weber, M.D. McCluskey, Formation of isolated Zn vacancies in ZnO single crystals by absorption of ultraviolet radiation: a combined study using positron annihilation, photoluminescence, and mass spectroscopy, Phys. Rev. Lett. 111 (2013) 017401.

[31] S.S. Park, J.M. Lee, S.J. Kim, S.W. Kim, M.S. Yi, S.H. Kim, S. Maeng, S. Fujita, ZnO nanotips and nanorods on carbon nanotube/Si substrates: anomalous p-type like optical properties of undoped ZnO nanotips, Nanotechnology 19 (2008) 245708.

[32] A. Travlos, N. Boukos, C. Chandrinou, H.S. Kwack, L.S. Dang, PL study of oxygen defect formation in ZnO nanorods, J. Appl. Phys. 106 (2009) 104307.

[33] B.G. Zhai, Y.M. Huang, Origin of thermal ‐ annealing induced orange emissions from solution–grown ZnO nanocrystals, Mater. Res. Innov. 19 S7 (2015) s45–s50.